Hindawi
Advances in Materials Science and Engineering
Volume 2022, Article ID 1047648, 9 pages
https://doi.org/10.1155/2022/1047648

Research Article

Effect of FNS Incorporation on the Properties of Ternary Blended Cement Containing Blast Furnace Slag and Fly Ash

Min Jae Kim,[1] **Eon Sang Park**,[2] **Woong Ik Hwang**,[3] **and Won Jung Cho**[3]

[1]*Department of Civil, Environmental and Architecture Engineering, Korea University, Seoul 02841, Republic of Korea*
[2]*Department of Construction System Engineering, Soongsil Cyber University, Seoul 03132, Republic of Korea*
[3]*Department of Civil and Environmental System Engineering, Hanyang University, Seoul 15588, Republic of Korea*

Correspondence should be addressed to Won Jung Cho; nelly91@hanyang.ac.kr

Received 22 December 2021; Revised 27 April 2022; Accepted 12 May 2022; Published 28 May 2022

Academic Editor: Nur Izzi Md Yusoff

This study aims to assess the properties of ternary blended concrete in terms of mechanical performance and resistance to chemical attack. Specimens consisted of concrete and paste having a water to binder ratio of 0.45 made with ordinary Portland cement, pozzolanic materials, and ferronickel slag. Results on compressive strength at l80 days of curing showed that ternary blended concrete with ferronickel slag was 8% to 18% higher than for OPC. For splitting tensile strength and flexural strength, however, there was no such trend. Durability was examined in terms of resistance to rapid chloride penetration, carbonation, and sulfate attack. Ternary mix showed always-higher resistance against chloride penetration and sulfate attack while being more susceptible to carbonation due to the lower pH of the cement matrix. In addition, all ternary mixes exhibited lower heat of hydration compared to OPC and binary mixes with pozzolanic materials showed the lowest heat evaporation. Furthermore, from the results of XRD analysis, identical hydration products were found irrespective to the binder, while a significant change was observed on the portlandite peak. Overall, results showed that the incorporation of ferronickel slag affected positively the properties of concrete.

1. Introduction

Since a number of national infrastructure facilities are made of concrete, the demand for concrete or the resources required to create it is not diminishing. Concrete deteriorates due to various physical and chemical factors during the period of use. When concrete structures lose their original function and thus cannot guarantee safety, it may cause an economic loss of the facility itself as well as damage of human life and property. For that reason, concrete structures must ensure safety, usability, and durability during the purposed lifetime in terms of physical performance and chemical resistance. The incorporating of other cementitious materials such as fly ash (PFA), ground granulated blast furnace slag (GGBS), or silica fume (SF) is one of the most typical methods to enhance the durability of concrete. The use of cementitious materials generally reduces the permeability of concrete against aggressive ions by densifying the cement matrix. This method is gaining popularity recently because using industrial by-products can also reduce the initial cost of construction and solve the environmental problems arising from the industrial by-products.

From the same point of view, an interest in ferronickel slag (FNS) has increased over the past decade. The FNS is a by-product generated in the process of synthesizing iron and nickel by melting them and consequently separating ferronickel [1, 2]. The production of FNS is estimated at about 2 million tons in Korea [1], 30 million tons in China [3], and approximately 3 million tons in Japan annually [4]. There was an effort to replace FNS as a construction material, for the last decades. For the first time, the use of FNS as a replacement for aggregates has been extensively conducted [2, 4–7], to resolve the depletion of natural aggregate. Recently, as the reactivity of FNS was confirmed, the utilization of FNS as a binder was also investigated [3, 5]. The FNS clinker reacts with $Ca(OH)_2$ in OPC (Ordinary Portland

Table 1: Chemical composition of the materials used in this study (%).

	CaO	SiO_2	Al_2O_3	MgO	Fe_2O_3	SO_3	K_2O	Na_2O_3	TiO_2
OPC	70.31	16.91	4.01	1.42	4.09	2.02	0.78	0.13	0.27
GGBS	47.18	29.70	13.13	4.55	0.64	2.29	0.52	0.22	1.11
PFA	3.93	65.48	18.48	0.64	5.81	0.80	1.45	1.29	1.12
FNS	6.28	48.23	3.59	23.01	15.76	0.50	0.09	-	0.11

Cement) to create secondary C-S-H gel, thereby contributing to the long-term strength development [8]. However, it has been still discussed whether FNS can provide a similar performance compared to conventional binders. Huang et al. [3] reported a reduction of compressive strength and chloride penetration resistance of FNS concrete than conventional OPC concrete. On the other hand, some research showed that the compressive strength of FNS incorporated mortars was similar to the PFA [1, 9]. Recently, economical or environmental advantages have been also reported through comparative analysis with conventional cementitious materials.

Though there have been a number of studies about the concrete mixed with FNS and OPC, research on ternary blended concrete is negligible. The ternary blended concrete has the advantage of complementing the limitation of each binder. In fact, owing to this benefit, there was an effort to use ternary blended concrete as a pavement material in Korea. However, the use of iron by-products with other conventional materials may raise unexpected harmful results on concrete structures [10]. Therefore, a precise analysis of the physical properties and durability should be accompanied for the ternary blended concrete containing FNS. Moreover, their properties must be taken into account in the concrete mixture design [11].

In this study, the term ternary blended concrete is defined as concrete that consists of FNS and GGBS or FNS and PFA in addition to OPC. The physical properties such as compressive strength, flexural strength, and splitting tensile strength were measured for concrete using blended cement in order to observe if there was any improvement. In addition, hydration characteristics were obtained through XRD analysis. Resistance to carbonation, chloride ion penetration, and sulfate attack were examined for durability evaluation. In concrete mixes, (OPC + GGBS or/and FNS) and (OPC + PFA or/and FNS) were partially admixed at 30% and 50% by weight of cement, respectively.

2. Materials and Methods

2.1. Materials. The Ordinary Portland Cement (OPC), Ground Granulated Blast Furnace Slag (GGBS), Pulverized Fuel Ash (PFA, class F), and ferronickel slag (FNS) were used for the binder. The fineness of OPC; GGBS; PFA, and FNS were 3,112; 3,800; 3,400, and 4,800 cm^2/g, respectively. The chemical compositions of used materials, measured by X-ray fluorescence (XRF), are given in Table 1. The main oxide components of FNS powder are SiO_2, MgO, and Fe_2O_3. Compared with PFA, the content of SiO_2 and Al_2O_3 is relatively low, but the content of CaO and Fe_2O_3 is higher. Other mixing materials consisted of distilled water, river sand (density: 2.45), and coarse aggregates (density: 3.17) with 25 mm of maximum size.

In order to identify the main clinker of raw materials, X-ray diffraction (XRD) curves of four different types of binders are given in Figure 1. The XRD curves of OPC mainly show alite ($3CaO•SiO_2$) and belite ($2CaOSiO_2$). GGBS showed a broad XRD curve, and peaks of belite and quartz were observed. On the other hand, PFA is mainly composed of crystalline quartz. The FNS, used in this study, was composed of forsterite (Mg_2SiO_4) and fayalite (Fe_2SiO_4) which also have a crystalline nature. Moreover, the XRD curve of FNS shows that MgO detected from XRF analysis are forsterite and fayalite, which usually show retarded hydration taking about 2 years to fully hydrate [12]. According to the oxide composition and XRD curve of FNS, the reactivity of FNS is expected to be lower than that of GGBS, but similar to PFA.

2.2. Mix Proportion. The detailed mix proportion, specimen type, and experimental program are suggested in Table 2. The OPC mix was selected as a control mixture, to investigate the influence of the incorporation of FNS and other conventional materials. In the binary formulation, the maximum amount of GGBS to be incorporated was 50%, and PFA was set to 25% according to the recommendation from the ACI committee [13, 14]. In the case of ternary blended mixtures, the FNS was substituted with half of the replaced amount of GGBS or PFA. The water-binder ratio was fixed to 0.45, irrespective of the binder type. No chemical admixture was added to exclude chemical reactivity with materials. The specimens were cured up to 1 year to achieve enough hydration of pozzolanic materials.

2.3. Test Method

2.3.1. Microscopic Examination. In order to investigate the hydration products of the ternary mix, cement paste was placed into a cubic mold ($50 \times 50 \times 10$ mm) after mixing with distilled water for 5 min and cured at room conditions ($20 \pm 2^{\circ}C$, RH $65 \pm 5\%$) for 24 hours. After that, specimens were demolded and stored in a water bath ($20 \pm 2^{\circ}C$) for previously defined ages. Then, the hardened paste specimens were fragmented or ground to make a proper specimen size for each microscopic examination.

To analyze the mineralogical composition of hydration products, XRD analysis using MDI JADE package software was employed on pastes after 365 days of curing. The scanning was carried out in the diffraction range (2θ) of

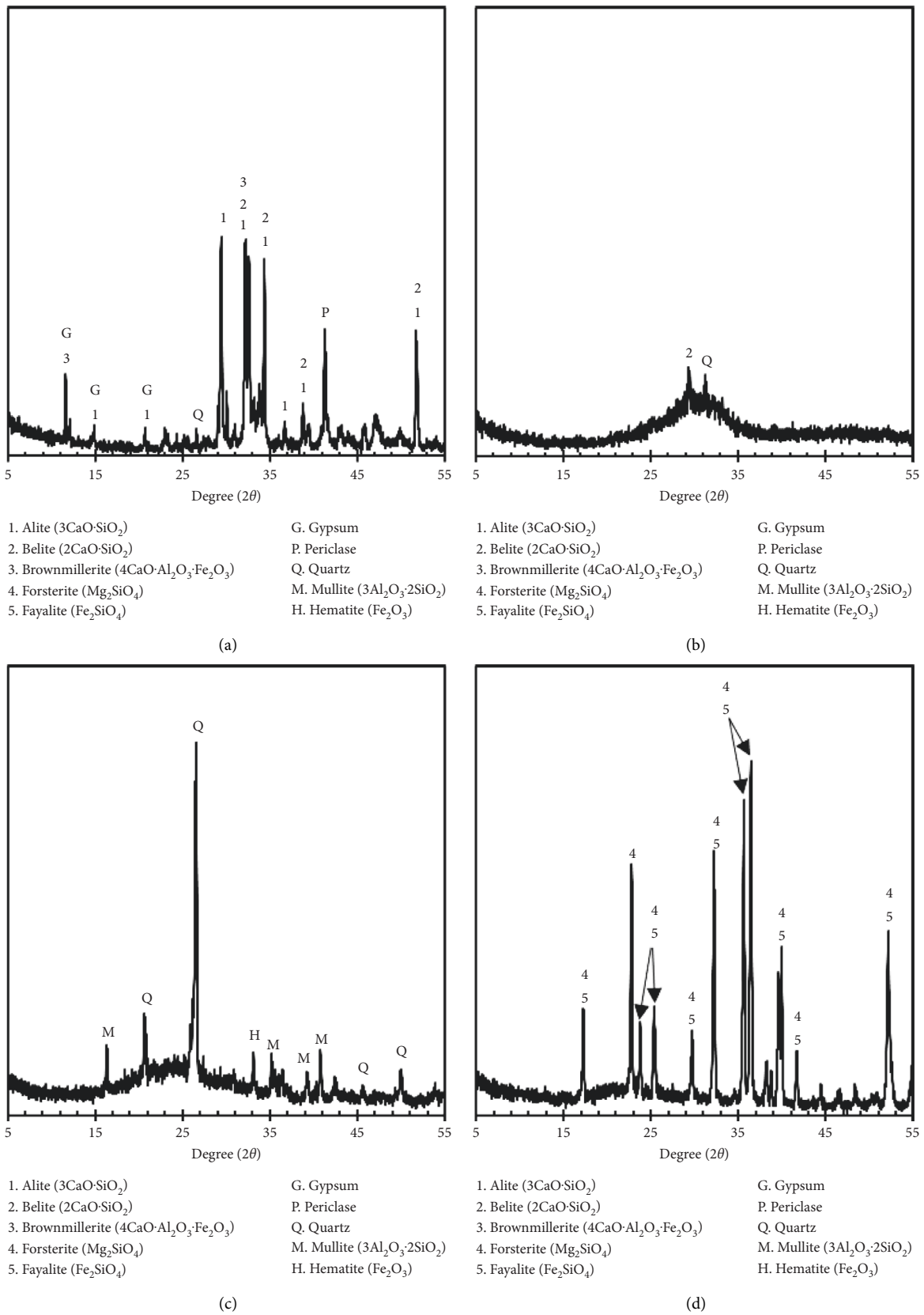

Figure 1: XRD curve for binders: (a) OPC, (b) GGBS, (c) PFA, and (d) FNS.

Table 2: Mix proportion and experiments (kg).

Type		OPC	FA	GGBS	FNS	Sand	Gravel	Water	Experiment
Paste	OPC	211	—		—	—	—		X-ray diffraction Mercury intrusion porosimetry
	OSP	160	—	160	—	—	—		
	OSN	160	—	80	80	—	—		
	OFA	148	52.8	—	—	—	—		
	OFN	148	26.4	—	26.4	—	—		
Concrete	OPC	778	—	—	—	1342	1890	0.45	Compressive strength
	OSP	598	—	180	—	915	934		Flexural strength
	OSN	598	—	90	90	917	935		Splitting tensile strength
	OFA	466	194.5	—	—	1348	1898		Carbonation depth
	OFN	466	97.25	—	97.25	1348	1898		Sulfate attack Chloride penetration resistance

5–60° at a rate of 4.0°/min with 40 kV voltage and 100 mA current with a wavelength of l.5405 A° (1 A° = 0.1 nm).

The pore structure characteristics of hardened cement paste were investigated by mercury intrusion porosimetry (MIP). After 365 days of curing, samples were dried in an oven at 50°C for 48 hours to stop further hydration. After then, the specimens were stored in acetone for 24 hours to eliminate the water in the pore. When the samples were placed in the MIP equipment, they were initially evacuated and the low pressure was generated up to 0.20 MPa by nitrogen gas. The specimen was subsequently intruded at pressures ranging from 3.7×10^{-3} to 413 MPa. The intrusion volume of Mercury was recorded at each corresponding pressure. The pore diameter was then derived by the Washburn equation as given in the following equation:

$$d = \frac{-4\gamma\cos\theta}{P}, \quad (1)$$

where d is the pore diameter (μm); γ is the surface tension (dynes/cm); P is the pressure (MPa); and θ is the contact angle (°) in which the present study took this value as 130°.

2.3.2. Mechanical Properties. Concrete cylinders (Ø 100 mm × 200 mm) were cast and cured for 7, 28, 56, 91, 180, and 365 days for the compressive strength test, followed by ASTM C39 [15]. Flexural strength was tested using a concrete specimen bar (100 × 100 × 400 mm) after 365 days of curing, conducted by third point load test according to ASTM C78 [16]. All the specimens-initiated fracture in the tension surface within the middle third of the span length and the rupture was calculated. Based on the ASTM C496 [17], cylindrical concrete specimens (Ø 150 mm × 300 mm) after 365 days of curing were used to measure the splitting tensile strength of concrete.

2.3.3. Durability of Blended Concrete. A rapid chloride permeability test (RCPT) was carried out according to ASTM C 1202 [18], by using slices of the concrete cylinder (Ø 100 mm × 50 mm) cured for 365 days. The electrical current passed through the specimen was measured every 30 min up to 6 hours. The voltage of 60 V DC was maintained across the ends of the concrete slice which were immersed between two chambers; one with 3% NaCl solution and the other with 0.3 M NaOH solution.

Sulfate attack was tested on matured concrete specimens (Ø100 mm × 200 mm) and cured until specified ages. The samples were submerged under 0.352 M Na_2SO_4 solution at 23 ± 2°C for 60 days. Then, weight change and loss of compressive strength were measured. This test method was determined by referring to the previous research [19, 20].

3. Results and Discussion

3.1. Microstructure Observation

3.1.1. XRD Analysis. The hydration products of FNS were identified by investigating the XRD curves of the cured paste samples. As given in Figure 2, the most abundant hydration products in the ternary mixed cement, at high peak intensities, were almost identical to the ones in OPC paste, such as portlandite and calcite. It seems that the long-term curing ages allowed forming calcite in all cement paste. Among the five types, OFA and OFN showed peak intensity of quartz, which is a clinker component of PFA. On the other hand, unreacted clinker was not detected in OSP and OSN. This is due to the fact that the lower content of CaO than GGBS contributed to initial hydration in fly ash inducing the remain of unreacted clinker. In the case of OSN and OFN, the content of unreacted FNS clinker so-called forsterite, and fayalite was also found. This is attributed to the late hydration characteristics of FNS when from OPC paste [21].

As shown in Figure 2(b), there is a distinct difference in the peak intensity for portlandite among the blended cement pastes. For example, the blended cement pastes have a lower value at the degree within 17.8–18.4° of 2θ, at which the main peak for portlandite is observed, while OPC shows strong intensity at the same degree range. The weakened intensity of peak for portlandite in the binary and ternary mix may be due to the latently hydraulic reaction in the cement matrix. In the OPC mix, in a highly alkaline environment, in fact, a partial replacement of PFA and GGBS particles would provide more C-S-H gel, resulting in a reduction peak of portlandite in the blended mix. For the case of OFA and OFN, the incorporation of PFA, however, induces a lower amount of portlandite, being attributed to delayed hydration. The peak intensity for unreacted PFA clinkers in the paste, in particular for quartz, is considerably high, indicating the hydration degree is lower at

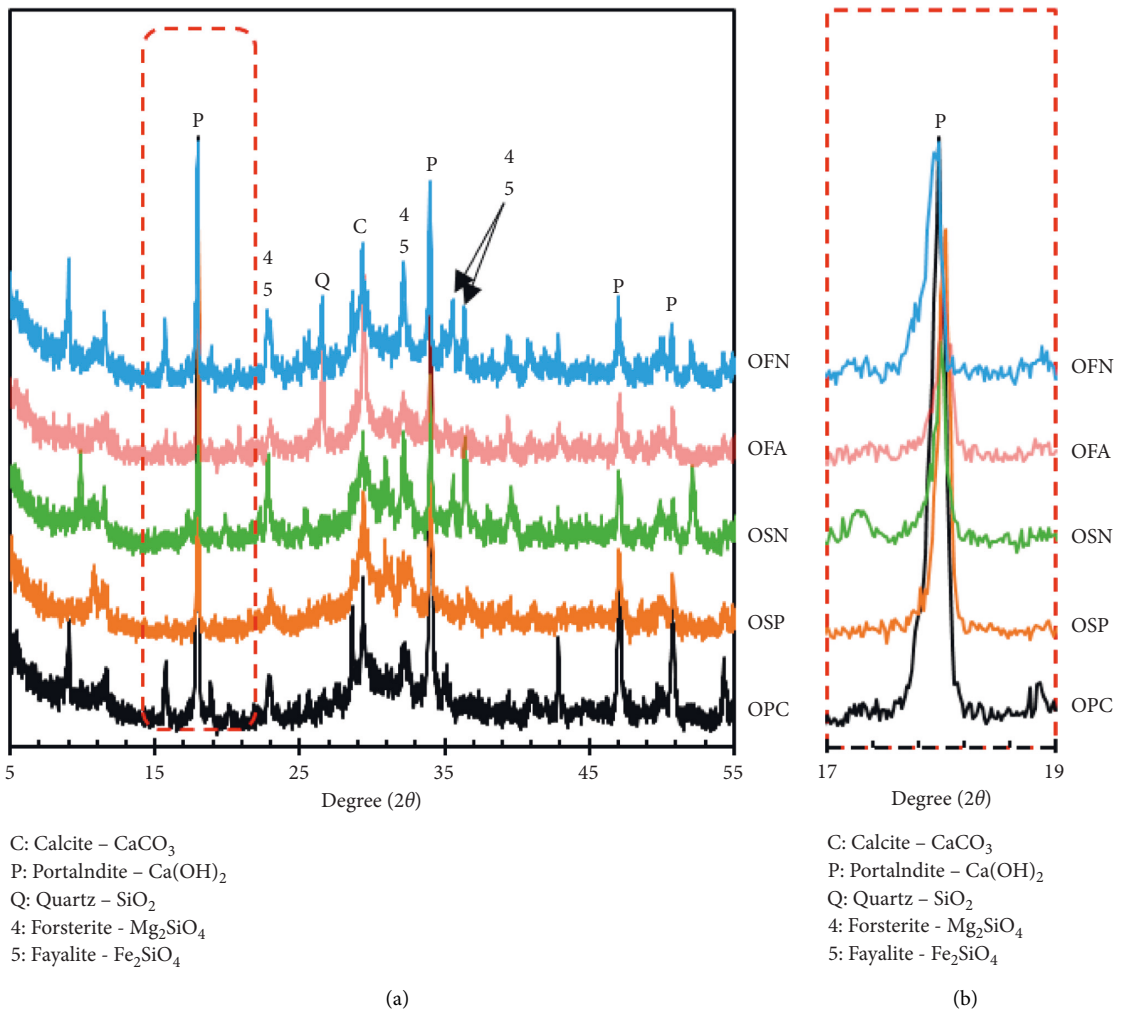

Figure 2: XRD curves of cement pastes cured at 365 days with different mix proportions: (a) whole patterns and (b) main peak for portlandite.

the given condition. On the other hand, the portlandite peak in the ternary blended cement is almost identical to the binary mix although unreacted FNS clinkers were also detected. This observation may mean that a lower intensity of portlandite in OSN and OFN samples is responsible for less hydration. Moreover, available space for hydration products can be provided by substitution of the lower hydraulic binder, FNS, at an identical W/B ratio so that acts as a nucleation site for the hydrates [22]. According to Huang et al. [3], Mg-bearing hydrates were not formed in the FNS-mixed pastes until 90 days. In this study, similarly, a formation of Mg/Fe-based phases originated from forsterite and fayalite in FNS, such as magnesium hydroxide ($Mg(OH)_2$; MH), was not observed. Therefore, the ternary blended specimen may be favorable to hydration arising from extra space in the matrix and would in turn form more C-S-H gel at 365 days of curing.

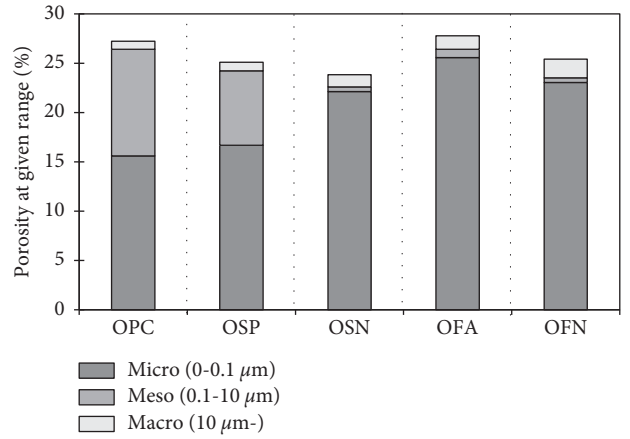

Figure 3: Mercury intruded volume at a given porosity for samples with different mix proportions cured for 365 days.

3.1.2. MIP Test Results. Pore size distributions for OPC, OSP, OSN, OFA, and OFN at the curing age of 365 days are shown in Figure 3. The range of pore size was categorized as follows [23]:

(1) Small-capillary (≤0.1 μm)
(2) Medium-capillary (0.1–10 μm)
(3) Macropores (large-capillary) (≥10 μm)

As for total pore volume, the curing age was crucial to all mixes. There was only a marginal difference for total porosity until a significant reduction at 365 days for all mixes, indicating 27.23, 25.11, 23.83, 27.78, and 25.40% for OPC, OSP, OSN, OFA, and OFN, respectively. When it comes to the pore distribution, OPC had the highest mesoporosity value accounting for 10.80%, while blended cement had 0.46–7.55%. Similarly, OSP showed relatively large mesoporosity compared to other blended samples. In turn, OSN showed the lowest total porosity (23.83%) and the highest microporosity about 22.12%. This phenomenon was again observed for OFA and OFN: 25.57 and 23.03% of microporosity at 365 days. It suggests that total porosity is largely influenced by mineral admixtures; in fact, an increase in the incorporation of FNS resulted in a decrease in alkalinity in the cement matrix and delayed the hydration process, presumably due to the refinement of the pore structure with the degree of hydration. Furthermore, the formation of C-S-H gel may represent the higher fraction of small-capillary pore, which is usually formed within the hydrates. Thus, the porosity of micropores would be increased with the incorporation of GGBS, PFA, and FNS as a binder. It has an important implication in that the lower pore diameter porosity could provide limited paths for aggressive ions and molecules to be mobile in the cement matrix.

3.2. Mechanical Properties

3.2.1. Development of Compressive Strength. Figure 4 represents the test results of compressive strength. The development of the compressive strength was strongly dependent on curing age and mix types. In fact, OPC was indicative of the highest compressive strength within 28 days, particularly accounting for 34.9 MPa at 28 days, whilst OSP, OSN, OFA, and OFN achieved 34.0, 33.0, 30.5, and 29.0 MPa, respectively. After 56 days, OSP had a higher compressive strength of about 42.5 MPa, compared to others with 37.0, 38.5, 36.75, and 33.5 MPa for OPC, OSN, OFA, and OFN, respectively. A rapid increase in the compressive strength for OSN and OFN in a long term may be, as expected, attributed to a latent hydration process of FNS. It is notable that OFA could not meet the strength with other blended concrete, which was subsequently achieved after 91 days, implying that further treatment could make OFA mix more feasible in situ by enhancing strength development at an early age, such as a reduction of a free water binder ratio and/or chemical admixture.

3.2.2. Mechanical Strength. To ensure applicability to fields, mechanical strengths were investigated for tensile and flexural strengths as given in Figure 5. As for splitting tensile and flexural strength, OPC ranked relatively the highest, followed by OSN, OSP OFN, and OFA. The splitting tensile strength was in the range of 2.86–3.17 MPa and the flexural strength was quite higher, accounting for 4.13–4.73 MPa at 365 days. Despite the lower level of tensile and flexural strengths for OFN and OFA, the margin for these strengths is allowable for structural concrete, considering that it accompanies a further reinforcement to compensate for the weakness. Moreover, it is notable that OSN achieved higher tensile and flexural strength than for OPC and OSP. It was observed in MIP test results that a concrete mix with FNS and GGBS represented the lowest total porosity but high porosity of micropores.

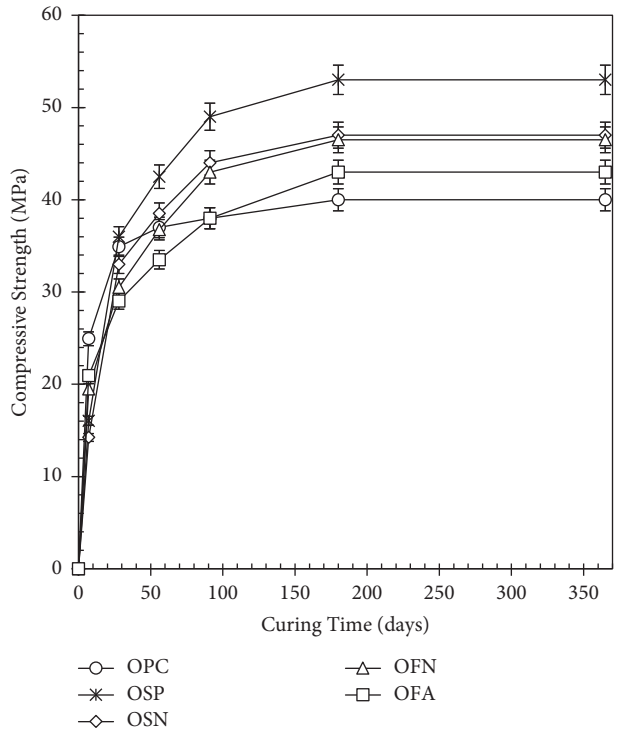

Figure 4: Development of compressive strength of concrete.

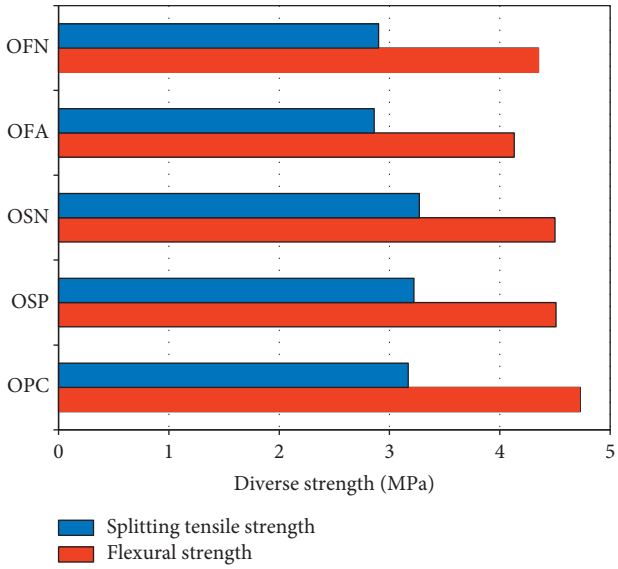

Figure 5: Mechanical strength of concrete at flexural and splitting tensile strengths.

3.3. Durability of Concrete

3.3.1. Chloride Ion Permeability. Rapid chloride penetration test (RCPT) results are given in Figure 6. It is evident that

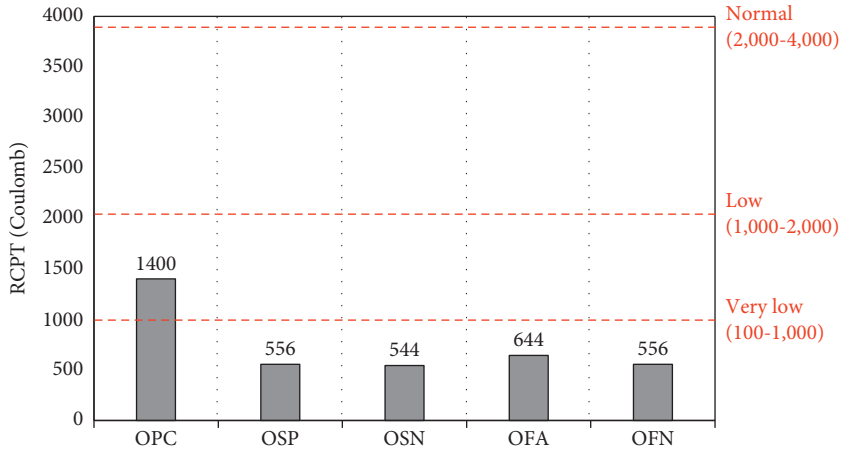

Figure 6: Resistance to chloride penetration.

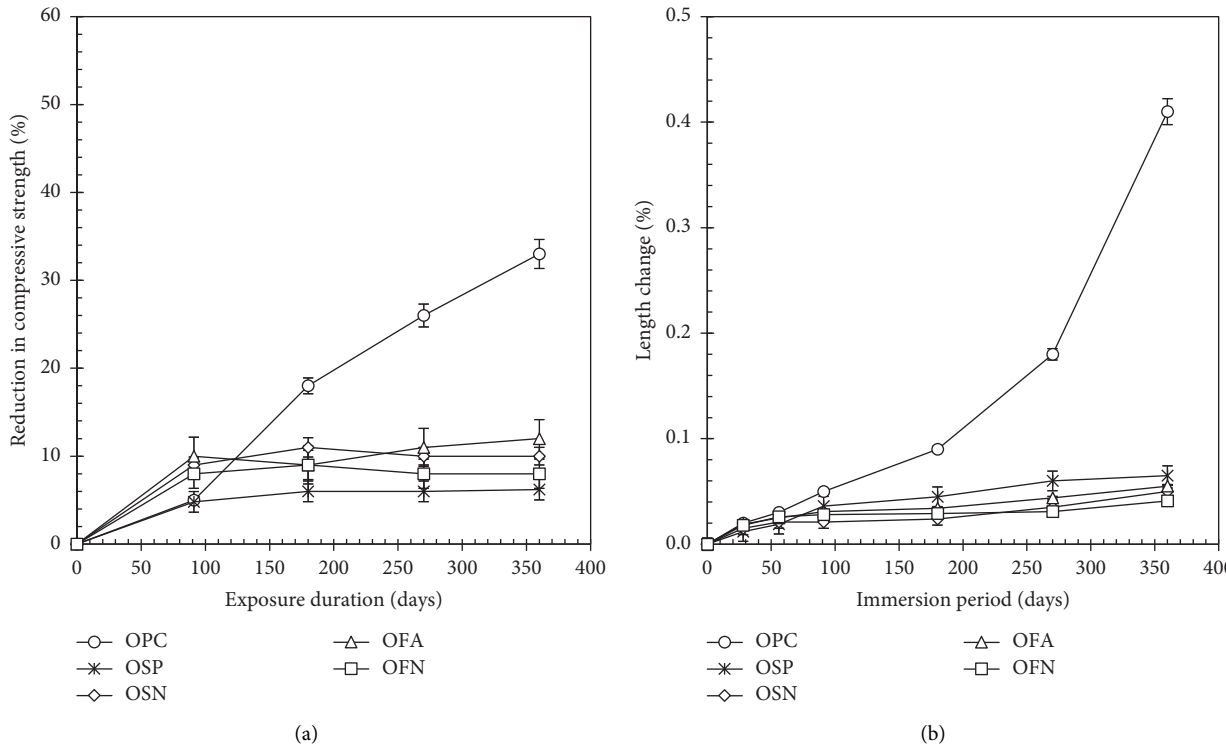

Figure 7: Resistance to sulfate attack of concrete.

OPC had the highest level of chloride ion penetrability, while OSP, OSN, OFA, and OFN imposed very low levels at identical conditions. It can be assumed that the mineral admixtures in the concrete mix reduced the critical pore size, implying that the pore structure in OSP, OSN, OFA, and OFN was mainly governed by a small capillary pore or/and gel pore, thereby leading to reduced ionic penetrability. However, the total porosity for OFA and OFN was even higher than OPC control as seen previously. It suggests that ionic transport in concrete is more influenced by pore distribution rather than pore volume; the higher volume for small capillary pore and gel pore may be beneficial in mitigating ionic transport at a given total porosity [19]. It is also notable that the charge passed for OSN and OFN were slightly lower in general than for OSP and OFA, presumably due to a further formation of micropores (i.e., gel pores), which had been significantly formed at exceeding 56 days of curing.

3.3.2. Resistance to Sulfate Attack. The degradation of concrete after sulfate attack for 91, 180, 270, and 365 days was examined by compressive strength reduction as shown in Figure 7(a). In terms of compressive strength, the reduction ratios were found to be 33.0, 6.2, 10.3, 12.1, and 8.0% for OPC, OSP, OSN, OFA, and OFN, respectively. The

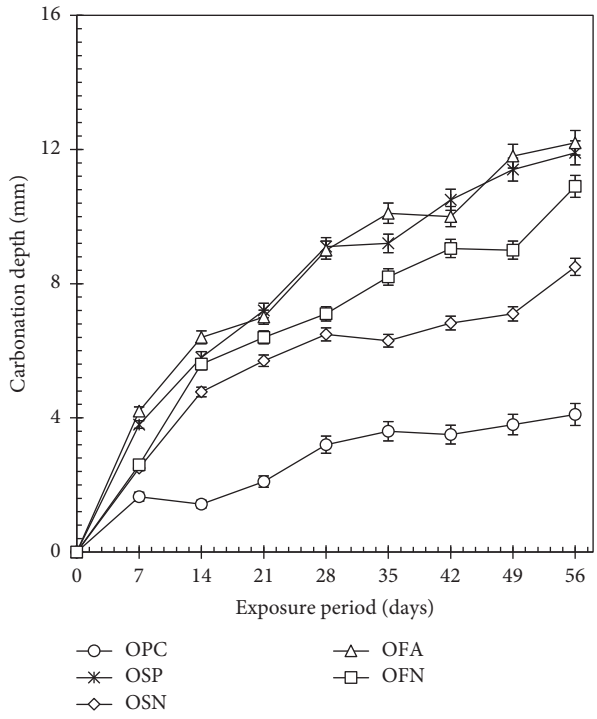

Figure 8: Carbonation depth for hardened concrete for 56 days.

length change of concrete specimens is also given in Figure 7(b).

Except for OPC, all types of blended cement showed high sulfate attack resistance. This experimental result was attributed to the change in the pore distribution of the cement matrix. It was confirmed that the incorporation of cementitious materials, such as PFA, GGBS, and FNS, made the pores denser than OPC. Due to the densified pore, the penetration of aggressive ions was blocked, and finally, degradation by sulfate was reduced. In fact, the tendency of compressive strength reduction ratio and length change shows similar results compare to the porosity test. Moreover, the incorporation of FNS may bring additional benefits to the resistance against sulfate attack. Tittelboom et al. [19] reported that delayed hydration of the FNS reduces the risk of sulfate attack by consuming the hydration products, which are needed to form the ettringite. Both OFN and OSN specimens showed a marginal change in the length change observation result.

3.3.3. Carbonation. To assess the resistance of ternary mix concrete to carbonation, concrete specimens were cured for 365 days and placed in the CO_2 chamber, of which the carbonation depth was determined by spraying the phenolphthalein solution as given in Figure 8. It is evident that the carbonation depth was simultaneously dependent on the exposure duration and mix types. At a very early age (7 days), the initial carbonation was developed to the depth of 1.65, 3.80, 2.50, 4.20, and 2.60 mm for OPC, OSP, OSN, OFA, and OFN, respectively and increased with time after 56 days to 4.10, 11.90, 8.50, 12.20, and 10.90 mm for corresponding mixes. As expected, OPC was the most resistive to carbonation, whilst OFN and OFA were the weakest presumably due to the chemically lower alkalinity. The lower alkalinity in OSP and OFA may arise from the higher portion of OPC replacement, of which the alkalinity in suspension conditions is often in the range of 8.0–9.0 in the pH, while for OPC it exceeds 12.5 up to 13.5 depending on the oxide composition. Moreover, the pore structure is also very crucial in determining the resistance to carbonation. In fact, total porosity would mainly govern the reactivity for carbonation, compared to other factors such as pore distribution, since gaseous CO_2 reaction occurs regardless of pore size. Although FNS incorporation concrete showed weak resistance to carbonation compared to OPC, unreacted crystalline FNS clinkers were attributed to pore refinement, thus it still showed lower carbonation depth and lower total porosity than the binary mix.

4. Conclusions

This section explains the main findings and implications of the work, highlighting its importance and relevance.

In this study, the main characteristics of five types of blended cement were assessed through experiments such as XRD analysis, MIP test, strength development, and chemical resistance. The hydration characteristic was also analyzed by XRD observation and pore structure analysis. The conclusion of this experiment is as follows:

(1) According to XRD analysis, a weakened intensity of portlandite peak was found in the binary and ternary mix cement compared to OPC. It is possibly due to the latently hydraulic reaction in the cement matrix. In the binary mix, a partial replacement of PFA and GGBS particles would provide more C-S-H gel, resulting in a reduction peak of portlandite. The portlandite peak in ternary blended cements are almost identical to binary mix and unreacted FNS clinkers were also detected. This observation suggested that by substitution of the lower hydraulic binder, FNS incorporation may be favorable to hydration arising from extra space in the matrix and would in turn form more C-S-H gel.

(2) The incorporation of FNS resulted in a decreased alkalinity in the cement matrix and delayed the hydration process, due to the refinement of the pore structure to denser pores at each degree of hydration. Moreover, the formation of C-S-H gel represents the higher fraction of small-capillary pore, which is usually formed within the hydrates.

(3) The development of compressive strength of blended mix is dependent on curing age as well as the replacement ratio. OSP showed improved performance compared to OPC, OSN, OFA, and OFN. Especially, a rapid increase of compressive strength was observed in FNS blended concrete in a long term due to the latent hydration process of FNS. The flexural and splitting tensile strength of blended concrete showed various trends compared to OPC,

being usually low, but still within the allowable margin for structural concrete

(4) The pore refinement in the FNS mix contributes to restricting the penetration of external aggressive ions thus resistance to chlorides ion penetration and sulfate attack would increase. However, due to the chemically lower alkalinity, blended concrete shows weaker carbonation resistance compared to OPC. [13].

Data Availability

The data presented in this study are available on request from the corresponding author.

Conflicts of Interest

The authors declare that they have no known conflicts of financial interest or personal relationships that could have appeared to influence the work reported in this paper.

Acknowledgments

This work was supported by the Korea Institute of Energy Technology Evaluation and Planning (KETEP) and the Ministry of Trade, Industry, and Energy (MOTIE) of the Republic of Korea: 20193210100050. The authors thank Prof K.Y. Ann (Hanyang University, South Korea) for the help of valuable discussion and experiment of ferronickel slag.

References

[1] B.-S. Cho, Y.-U. Kim, D.-B. Kim, and S.-J. Choi, "Effect of ferronickel slag powder on microhydration heat, flow, compressive strength, and drying shrinkage of mortar," *Advances in Civil Engineering*, vol. 2018, Article ID 6420238, 7 pages, 2018.

[2] Y. C. Choi and S. Choi, "Alkali-silica reactivity of cementitious materials using ferro-nickel slag fine aggregates produced in different cooling conditions," *Construction and Building Materials*, vol. 99, pp. 279–287, 2015.

[3] Y. Huang, Q. Wang, and M. Shi, "Characteristics and reactivity of ferronickel slag powder," *Construction and Building Materials*, vol. 156, pp. 773–789, 2017.

[4] Y. Sakoi, M. Aba, Y. Tsukinaga, and S. Nagataki, "Properties of concrete used in ferronickel slag aggregate," in *Proceedings of the 3rd International Conference on Sustainable Construction Materials and Technologies*, Tokyo, Japan, August 2013.

[5] K. KoNubu and M. Shoya, "Guidelines for construction using Ferronickel slag fine aggregate concrete," *Concrete library of JSCE*, vol. 24, 1994.

[6] A. K. Saha and P. K. Sarker, "Compressive strength of mortar containing ferronickel slag as replacement of natural sand," *Procedia Engineering*, vol. 171, pp. 689–694, 2017.

[7] A. K. Saha and P. K. Sarker, "Expansion due to alkali-silica reaction of ferronickel slag fine aggregate in OPC and blended cement mortars," *Construction and Building Materials*, vol. 123, pp. 135–142, 2016.

[8] N. Lemonis, P. E. Tsakiridis, N. S. Katsiotis et al., "Hydration study of ternary blended cements containing ferronickel slag and natural pozzolan," *Construction and Building Materials*, vol. 81, pp. 130–139, 2015.

[9] M. A. Rahman, P. K. Sarker, F. U. A. Shaikh, and A. K. Saha, "Soundness and compressive strength of Portland cement blended with ground granulated ferronickel slag," *Construction and Building Materials*, vol. 140, pp. 194–202, 2017.

[10] A. Qi, X. Liu, Z. Wang, and Z. Chen, "Mechanical properties of the concrete containing ferronickel slag and blast furnace slag powder," *Construction and Building Materials*, vol. 231, Article ID 117120, 2020.

[11] I. Papayianni and E. Anastasiou, "Production of high-strength concrete using high volume of industrial by-products," *Construction and Building Materials*, vol. 24, no. 8, pp. 1412–1417, 2010.

[12] E. Bernard, B. Lothenbach, D. Rentsch, I. Pochard, and A. Dauzères, "Formation of magnesium silicate hydrates (M-S-H)," *Physics and Chemistry of the Earth, Parts A/B/C*, vol. 99, pp. 142–157, 2017.

[13] D. Suresh and K. Nagaraju, "Ground granulated blast slag (GGBS) in concrete–a review," *IOSR Journal of Mechanical and Civil Engineering*, vol. 12, no. 4, pp. 76–82, 2015.

[14] ACI Committee 211, *ACI 211.1-91 (Reapproved 2009) Standard Practice for Selecting Proportions for Normal, Heavyweight, and Mass Concrete*, American Concrete Institute, Farmington Hill, Farmington Hills, MI, USA, 2009.

[15] ASTM International Committee C-9 on Concrete and Concrete Aggregates, *Standard Test Method for Compressive Strength of Cylindrical Concrete Specimens*, ASTM international, Pennsylvania, PA, USA, 2014.

[16] ASTM, C78, "Standard test method for flexural strength of concrete (using simple beam with third-point loading)," *American Society for Testing and Materials*, vol. 100, p. 5, 2010.

[17] A. Astm, "ASTM C496/C496M-04e1 Standard Test Method for Splitting Tensile Strength of Cylindrical Concrete Specimens," *Annual book of ASTM standards*, vol. 4, 2008.

[18] American Society for Testing and Materials. Committee C-9 on Concrete and Concrete Aggregates. Standard Test Method for Electrical Indication of Concrete's Ability to Resist Chloride Ion Penetration. ASTM International, Pennsylvania, PA, USA, 2012.

[19] K. V. Tittelboom, N. De Belie, and R. D. Hooton, "Test methods for resistance of concrete to sulfate attack—a critical review," *RILEM State-of-the-Art Reports*, vol. 10, pp. 251–288, 2013.

[20] Y.-S. Park, J.-K. Suh, J.-H. Lee, and Y.-S. Shin, "Strength deterioration of high strength concrete in sulfate environment," *Cement and Concrete Research*, vol. 29, no. 9, pp. 1397–1402, 1999.

[21] H. Kim, C. H. Lee, and K. Y. Ann, "Feasibility of ferronickel slag powder for cementitious binder in concrete mix," *Construction and Building Materials*, vol. 207, pp. 693–705, 2019.

[22] B. Lothenbach, K. Scrivener, and R. D. Hooton, "Supplementary cementitious materials," *Cement and Concrete Research*, vol. 41, no. 12, pp. 1244–1256, 2011.

[23] S. Mindess, J. F. Young, and D. Darwin, *Concrete*, Prentice-Hall, New Jersy, NJ, USA, Second Edition, 2002.